

# Binding Energies of Protonated Betaine Complexes: A Probe of Zwitterion Structure in the Gas Phase

William D. Price, Rebecca A. Jockusch, and Evan R. Williams\*

Contribution from the Department of Chemistry, University of California, Berkeley, California, 94720

Received July 25, 1997

**Abstract:** The dissociation kinetics of proton-bound dimers of betaine with molecules of comparable gas-phase basicity were investigated using blackbody infrared radiative dissociation (BIRD). Threshold dissociation energies were obtained from these data using master equation modeling. For bases that have comparable or higher gas-phase basicity, the binding energy of the protonated base•betaine complex is  $\sim 1.4$  eV. For molecules that are  $\sim 2$  kcal/mol or more less basic, the dissociation energy of the complexes is  $\sim 1.2$  eV. The higher binding energy of the former is attributed to an ion–zwitterion structure which has a much larger ion–dipole interaction. The lower binding energy for molecules that are  $\sim 2$  kcal/mol or more less basic indicates that an ion–molecule structure is more favored. Semiempirical calculations at both the AM1 and PM3 levels indicate the most stable ion–molecule structure is one in which the base interacts with the charged quaternary ammonium end of betaine. These results indicate that the measurement of binding energies of neutral molecules to biological ions could provide a useful probe for the presence of zwitterions and salt bridges in the gas phase. From the BIRD data, the gas-phase basicity of betaine obtained from the kinetic method is found to be  $239.2 \pm 1.0$  kcal/mol. This value is in excellent agreement with the value of 239.3 kcal/mol (298 K) from ab initio calculations at the MP2/6-31+g\*\* level. The measured value is slightly higher than those reported previously. This difference is attributed to entropy effects. The lower ion internal energy and longer time frame of BIRD experiments should provide values closer to those at standard temperature.

## Introduction

Salt-bridge and zwitterion structures are known to play a crucial role in the structure, function, and activity of proteins and peptides in solution. The contribution of these strong electrostatic interactions in the gas-phase chemistry of biomolecule ions is less well established. Both experimental<sup>1–3</sup> and theoretical<sup>4–8</sup> evidence suggests that zwitterionic conformers of glycine and small peptides consisting of glycine and alanine are not stable in the gas phase. However, recent investigations indicate that salt bridges are important factors in the conformation, reactivity, and dissociation mechanisms of gas-phase peptides<sup>3,9–14</sup> and proteins.<sup>15,16</sup> Salt bridges have been proposed to play a role in gas-phase H/D exchange<sup>3</sup> and in producing

specific backbone cleavages at acidic residues in proteins.<sup>15,16</sup> The singly protonated gas-phase bradykinin ion has been shown to form a stable salt-bridge structure between the two protonated terminal arginine side chain residues and the deprotonated C-terminus carboxyl group.<sup>9</sup> Modeling suggests that the polar groups of this ion, primarily the carbonyl oxygens of the peptide backbone, form an intramolecular solvent shell that stabilizes the separated charges.<sup>17</sup>

Gas-phase salt bridges in biomolecules may be favorable even without significant intramolecular solvation. Recent evidence suggests that protonated dimers of the amino acid arginine are bound by a salt bridge, i.e., an ion–zwitterion interaction, but dimers of glycine are bound by a simple ion–molecule interaction.<sup>18</sup> This conclusion was deduced on the basis of differences in binding energies of these amino acid complexes and the corresponding methyl esters. An interaction between an ion and a zwitterion with a very large permanent dipole moment is expected to be stronger than that between an ion and a neutral molecule with a significantly smaller dipole moment. Thus, measurement of binding energies of ion–molecule complexes may provide a useful probe for the presence of zwitterions and salt bridges in gas-phase biomolecule ions.

Betaine [(CH<sub>3</sub>)<sub>3</sub>N<sup>+</sup>CH<sub>2</sub>COO<sup>-</sup>], a methylated derivative of the amino acid glycine, is widely distributed in plant and animal tissues and is a naturally occurring zwitterion. Gas-phase

\* To whom correspondence should be addressed.

- (1) Suenram, R. D.; Lovas, F. J. *J. Mol. Spectrosc.* **1980**, *72*, 372–382.
- (2) Locke, M. J.; McIver, R. T., Jr. *J. Am. Chem. Soc.* **1983**, *105*, 4226–4232.
- (3) Campbell, S.; Rodgers, M. T.; Marzluff, E. M.; Beauchamp, J. L. *J. Am. Chem. Soc.* **1995**, *117*, 12840–12854.
- (4) Gordon, M. S.; Jensen, J. H. *Acc. Chem. Res.* **1996**, *29*, 536–543.
- (5) Ding, Y. B.; Krogh-Jespersen, K. *Chem. Phys. Lett.* **1992**, *199*, 261–266.
- (6) Csaszar, A. G. *J. Am. Chem. Soc.* **1992**, *114*, 9568–9575.
- (7) Yu, D.; Armstrong, D. A.; Rauk, A. *Can. J. Chem.* **1992**, *70*, 1762–1772.
- (8) Wright, L. R.; Borkman, R. F. *J. Phys. Chem.* **1982**, *86*, 3956–3962.
- (9) Schnier, P. D.; Price, W. D.; Jockusch, R. A.; Williams, E. R. *J. Am. Chem. Soc.* **1996**, *118*, 7178–7189.
- (10) Gonzalez, J.; Besada, V.; Garay, H.; Reyes, O.; Padron, G.; Tambara, Y.; Takao, T.; Shimonishi, Y. *J. Mass Spectrom.* **1996**, *31*, 150–158.
- (11) Grese, R. P.; Cerny, R. L.; Gross, M. L. *J. Am. Chem. Soc.* **1989**, *111*, 2835–2842.
- (12) Deery, M. J.; Summerfield, S. G.; Buzy, A.; Jennings, K. R. *J. Am. Chem. Soc. Mass Spectrom.* **1997**, *8*, 253–261.
- (13) Cox, K. A.; Gaskell, S. J.; Morris, M.; Whiting, A. *J. Am. Chem. Soc. Mass Spectrom.* **1996**, *7*, 522–531.

(14) Summerfield, S. G.; Whiting, A.; Gaskell, S. J. *Int. J. Mass Spectrom. Ion Processes* **1997**, *162*, 149–161.

(15) Price, W. D.; Schnier, P. D.; Jockusch, R. A.; Strittmatter, E. F.; Williams, E. R. *J. Am. Chem. Soc.* **1996**, *118*, 10640–10644.

(16) Jockusch, R. A.; Schnier, P. D.; Price, W. D.; Strittmatter, E. F.; Demirev, P. A.; Williams, E. R. *Anal. Chem.* **1997**, *69*, 1119–1126.

(17) Wyttenbach, T.; von Helden, G.; Bowers, M. T. *J. Am. Chem. Soc.* **1996**, *118*, 8355–8364.

complexes of protonated ions with betaine are excellent prototypes for quantifying salt-bridge interactions. The thermochemical properties of model betaine complexes can provide considerable insight into the ion-zwitterion interactions observed in gas-phase biomolecules. Using the kinetic method, Cooks and co-workers<sup>19</sup> have recently measured the gas-phase basicity (GB) of betaine as  $232.9 \pm 0.8$  kcal/mol from which a gas-phase proton affinity (PA) of 239.8 kcal/mol was estimated. Beauchamp and co-workers<sup>20</sup> obtained a PA of 242 kcal/mol using an FT-ICR mass spectrometer, consistent with a value of 241.3 kcal/mol calculated at the PM3 level.<sup>3</sup> These pioneering experiments provide the first measure of the GB of a zwitterion compound. The GB of the conjugate base of glycine is 335.1 kcal/mol.<sup>21</sup> The large difference in GB for these structurally similar compounds is consistent with the stabilization due to Coulombic attraction between the trimethylammonium cation and the carboxylic anion.<sup>19</sup>

The potential energy surface for H/D exchange between betaine and NH<sub>3</sub> has been reported by Beauchamp and co-workers.<sup>3</sup> Calculations at the PM3 semiempirical level model the energetic requirements of a proposed salt-bridge mechanism applicable to H/D exchange between a deuterated reagent gas and the carboxyl hydrogen in protonated glycine oligomers. These calculations show the complex formed between neutral NH<sub>3</sub> and protonated betaine is 12.6 kcal/mol more stable than the separated reactants. However, the ion-zwitterion complex formed by transferring a proton from betaine to NH<sub>3</sub> is stabilized by an additional 5.4 kcal/mol.

A new thermal dissociation technique, blackbody infrared radiative dissociation (BIRD), has recently been applied to a variety of gas-phase biomolecule ions<sup>9,15,16,22–24</sup> and proton-bound dimers.<sup>18,25</sup> Ions stored in a Fourier transform mass spectrometer can be activated by absorbing blackbody photons from the heated vacuum chamber walls. At pressures below  $2 \times 10^{-8}$  Torr, the dissociation kinetics are independent of the vacuum chamber pressure (the zero-pressure limit). From the temperature dependence of the unimolecular dissociation constants ( $k_{\text{uni}}$ ), Arrhenius activation parameters in the zero-pressure limit can be obtained. This was first demonstrated by McMahon and co-workers<sup>26,27</sup> for small weakly bound cluster ions. Dunbar<sup>28,29</sup> showed that the internal energy distribution of these ions was similar to a Boltzmann distribution, but truncated at the high-energy tail. Measured Arrhenius activation energies ( $E_a$ ) for these small weakly bound complexes are smaller than values obtained from a true Boltzmann distribution of ions

( $E_a^\infty$ ). The threshold dissociation energy ( $E_0$ ) for these ions can be obtained by adding a correction factor to the measured  $E_a$ . Large ions can exchange photons with the blackbody field at rates much faster than they dissociate. In this rapid energy exchange (REX) limit, the internal energy of the reacting population of ions is given by a Boltzmann distribution at the temperature of the vacuum chamber.<sup>15,30</sup> True values of the Arrhenius activation energy ( $E_a^\infty$ ) and preexponential factor ( $A^\infty$ ) are measured and can be directly related to the threshold dissociation energy ( $E_0$ ) and the entropy of transition, respectively, via transition state theory. For intermediate-sized ions, such as the proton-bound dimers of amino acids, the internal energy distribution is Boltzmann-like but partially depleted at higher energies.<sup>25</sup> Measured Arrhenius parameters are less than the REX limit values. Master equation modeling is necessary to extract  $E_0$  from the measured  $E_a$ .

Here, dissociation kinetics of protonated dimers of betaine with a series of reference compounds of known GB are measured using BIRD. Threshold dissociation energies are obtained from these data by master equation modeling. Information about the structure of these complexes is deduced from the correlation between the dissociation energy and the GB of the reference compound.

## Experimental Section

**Mass Spectrometry.** A Fourier transform mass spectrometer with a 2.7 T superconducting magnet and an external electrospray ionization source was used for all BIRD measurements.<sup>22,31</sup> Ions generated in the external source are guided by a series of electrostatic lenses through five stages of differential pumping into the ion cell. The efficiency of ion trapping and thermalization is enhanced by introducing  $\sim 10^{-6}$  Torr of dry nitrogen through a pulsed valve into the heated vacuum chamber. Ion accumulation time is varied between 1.5 and 15 s to optimize the signal. A mechanical shutter in the ion beam path is opened during the ion accumulation event and subsequently closed to prevent both ion and neutral molecules, originating in the electrospray source, from being introduced into the ion cell during the reaction delay. A 5 s pump-down delay follows the ion accumulation. The pressure in the FTMS cell is between 5 and  $8.5 \times 10^{-9}$  Torr at all chamber temperatures, except for the heterodimers of betaine with TBA and DMPA where the pressure was  $1.5\text{--}2.0 \times 10^{-8}$  Torr. Dimer ions are subsequently isolated by using both stored waveform inverse Fourier transform (SWIFT)<sup>32</sup> and single radio frequency ejection. Isolated dimer ions are then allowed to dissociate for times up to 600 s. Data are collected with a Finnigan Odyssey data system at an acquisition rate of 2286 kHz ( $m/z$  36 cutoff), and 128K data points are stored. A broad-band radio frequency sweep rate of 3200 Hz/ $\mu$ s (120 V p-p) is used to excite ions for detection.

The main vacuum chamber, located within the solenoid of the superconducting magnet and containing the ion cell, is heated by a direct current resistive heating blanket. The temperature is controlled by an Omega proportioning temperature controller to within  $\pm 0.5$  °C. The vacuum chamber on both sides of the superconducting magnet are separately heated to within  $\pm 5$  °C of the central portion. The temperature of the ion cell was monitored with three copper-constantan thermocouples, one adjacent to each excite plate and one mounted on one of the stainless steel bars used to support the FTMS cell. These thermocouples have been calibrated to one previously placed in the center of the cell. All temperatures reported here correspond to the temperature at the center of the cell.

**Materials.** All reagents were purchased from Aldrich Chemical Co. (Milwaukee, WI) and were used without further purification. The

(18) Price, W. D.; Jockusch, R. A.; Williams, E. R. *J. Am. Chem. Soc.* **1997**, *119*, 11988–11989.

(19) Patrick, J. S.; Yang, S. S.; Cooks, R. G. *J. Am. Chem. Soc.* **1996**, *118*, 231–232.

(20) From ref 19: Beauchamp, J. L. Presented at the 209th National Meeting of the American Chemical Society, Anaheim, CA, April 2–7, 1995.

(21) Lias, S. G.; Bartness, J. E.; Liebman, J. F.; Holmes, J. L.; Levin, R. D. Gas-Phase Ion Neutral Thermochemistry. *J. Phys. Chem. Ref. Data* **1988**, *17*, Suppl. 1.

(22) Price, W. D.; Schnier, P. D.; Williams, E. R. *Anal. Chem.* **1996**, *68*, 859–866.

(23) Schnier, P. D.; Price, W. D.; Strittmatter, E. F.; Williams, E. R. *J. Am. Soc. Mass Spectrom.* **1997**, 771–780.

(24) Gross, D. S.; Zhao, Y.; Williams, E. R. *J. Am. Soc. Mass Spectrom.* **1997**, *8*, 519–524.

(25) Price, W. D.; Schnier, P. D.; Williams, E. R. *J. Phys. Chem. B* **1997**, *101*, 664–673.

(26) Thölmann, D.; Tonner, D. S.; McMahon, T. B. *J. Phys. Chem.* **1994**, *98*, 2002–2004.

(27) Tonner, D. S.; Thölmann, D.; McMahon, T. B. *Chem. Phys. Lett.* **1995**, *233*, 324–330.

(28) Dunbar, R. C. *J. Phys. Chem.* **1994**, *98*, 8705–8712.

(29) Dunbar, R. C.; McMahon, T. B.; Thölmann, D.; Tonner, D. S.; Salahub, D. R.; Wei, D. *J. Am. Chem. Soc.* **1995**, *117*, 12819–12825.

(30) Price, W. D.; Williams, E. R. *J. Phys. Chem. A* **1997**, *101*, 8844–8852.

(31) Gross, D. S.; Williams, E. R. *J. Am. Chem. Soc.* **1995**, *117*, 883–890.

(32) Marshall, A. G.; Wang, T. C.; Ricca, T. L. *J. Am. Chem. Soc.* **1985**, *107*, 7893–7897.

homodimer of betaine and heterodimers of betaine with DBU, DBN, DMPA, TBA, and TMG are formed directly by electrospray from  $\sim 10^{-4}$  M 90:10 methanol/water solutions. Cross dimer solutions are formed by mixing the  $10^{-4}$  M stock solution of betaine with the respective bases in a ratio that optimizes the dimer signal. Heterodimers of betaine with TMDP and TMDB could not be formed directly by electrospray. To form these dimers, a  $\sim 10^{-4}$  M 50:50 methanol/water betaine solution was electrosprayed into a low flow countercurrent of dry  $N_2$  gas that was bubbled through the respective base. Presumably, stabilized heterodimers are formed when protonated gas-phase betaine collides with neutral base molecules either prior to entering or in the heated capillary interface.

**Calculations of Vibrational Frequencies and Transition Dipole Moments.** An ensemble of low-energy structures for each dimer was calculated by molecular modeling using the consistent valence force field (CVFF) provided in the Insight/Discover suite of programs (Biosym Technologies, San Diego, CA) on a Silicon Graphics solid impact 10000 computer. Because of their higher gas-phase basicity, the proton is placed on DBN and DBU for dimers containing these constituents. The proton is placed on a carboxyl oxygen of betaine for the DMPA, TBA, TMDP, and TMDB heterodimers and the betaine homodimer. The proton-bound dimers of TMG and betaine (TMG-betaine) are separately modeled with the proton on either betaine or TMG. For dimers containing zwitterionic betaine (homodimer and heterodimers containing DBN, DBU, and TMG), molecular dynamics are run at 600 K for 6 ps followed by simulated annealing to 200 K over 3 ps and then energy minimized to a 0 K structure. All classical trajectories are integrated over a 1 fs step size. This 0 K structure was then used to initiate a new dynamics cycle. This process was repeated 120 times for each dimer. In the dynamics simulations, heterodimers in which betaine is protonated (heterodimers containing DMPA, TBA, TMDP, TMDB, and TMG) were found to dissociate at temperatures greater than 350 K. For these dimers, dynamics are run at 350 K for 4 ps. The lowest energy geometry found for each dimer is used as the starting coordinates for AM1 semiempirical calculations using MOPAC 6.0, also on an SGI solid impact 10000 computer. Full electronic structure minimization using the eigenvector following routine was performed. Vibrational frequencies ( $\nu$ ) and transition dipole moments ( $\mu$ ) are calculated from these minimized structures.

The enthalpy of formation for several conformations of the TMG-betaine heterodimer are calculated at both the AM1 and PM3 semiempirical levels. The lowest energy MD geometries are used as initial coordinates for both the ion-zwitterion and ion-molecule complexes. Additional ion-molecule structures are constructed by coordinating the TMG nitrogen lone pair electrons with methyl groups of the charged quaternary end of protonated betaine. These structures are energy minimized with molecular mechanics (CVFF) prior to semiempirical electronic structure optimization.

**Master Equation.** A complete description of our implementation of the master equation is given elsewhere.<sup>25</sup> A discrete value finite-difference formulation of the master equation was used to model the dissociation of these dimers. The complete set of coupled differential equations describing the time evolution of a dissociating population of ions can be written in a matrix form (**J** matrix). The **J** matrix contains the detailed rate constants for all radiative energy transfer and dissociation processes, and its solution simulates the BIRD experiment. In the zero-pressure limit, applicable to these experiments, the energy transfer processes are described completely by the rates of absorption ( $k_{1,\text{rad}}$ ) and emission ( $k_{-1,\text{rad}}$ ) of blackbody photons:

$$k_{1,\text{rad}}(\Delta E_{i-j} = h\nu) = \sum_m \rho(h\nu) \mathbf{B}(h\nu) P_i^{m,h\nu} \quad (1)$$

$$k_{-1,\text{rad}}(\Delta E_{j-i} = h\nu) = \sum_m \{\mathbf{A}(h\nu) + \rho(h\nu) \mathbf{B}(h\nu)\} P_j^{m,h\nu} \quad (2)$$

where  $\rho(h\nu)$  is the energy density of the blackbody field given by the Planck distribution.  $\mathbf{A}(h\nu)$  and  $\mathbf{B}(h\nu)$  are the Einstein coefficients for stimulated and spontaneous radiative processes, respectively, given by

$$\mathbf{B}(h\nu) = \mu^2/6\epsilon_0 \hbar^2 \quad (3)$$

$P_j^{m,h\nu}$  is the product of the probability of the  $\nu$ th oscillator containing  $m$

$$\mathbf{A}(h\nu) = 8\pi h(\nu/c)^3 \mathbf{B}(h\nu) \quad (4)$$

quanta of energy and the enhanced probability of a radiative transition from an excited harmonic oscillator. The microcanonical dissociation rate constants are calculated from RRKM theory. Transition state frequency sets are assembled from the reactant frequencies by removing the stretching mode between the monomer units (typically 2200–2500  $\text{cm}^{-1}$ ), and systematically varying five additional frequencies to lower values. The sum and density of states are calculated using the efficient and exact Beyer-Swinehart algorithm. Angular momentum is not rigorously conserved, and internal rotations are treated as low-frequency vibrations. These approximations are not expected to adversely affect these calculations.<sup>33,34</sup>

The finite-difference solution to the master equation requires an energy distribution of the initial ion population. A Boltzmann distribution was used for all these calculations. However, the steady-state reactant population is independent of the initial distribution. The steady-state distribution is Boltzmann-like, but is depleted at the higher energy levels. Following the establishment of a steady-state population, the unimolecular dissociation rate constant ( $k_{\text{uni}}$ ) is evaluated from the slope of  $\ln\{\text{unreacted population}\}$  vs time. These rate constants are calculated at the two extremes of the experimental temperature range for each dimer complex, and an  $E_a$  and  $A$  are determined.

All master equation modeling was performed with software developed in this laboratory using double-precision Fortran 77 code on a SUN Enterprise 5000 computer. The NAG Mark 17 library routine DO2NCF, the backward differentiation formula for solving stiffly coupled differential equations, is used to facilitate **J** matrix integration.

**Molecular Orbital Calculations.** Ab initio level calculations on betaine and protonated betaine monomers were done using GAUSSIAN 92 (Gaussian, Inc., Pittsburgh, PA) to calculate the PA and GB of betaine. A low-energy ensemble of structures for each was found using the same molecular dynamics routine described for the betaine dimer. Geometry optimization at the AM1 level was performed on the lowest energy MD structure. These structures are then used as initial coordinates for full electronic structure optimization performed successively at the RHF/6-31g\*, RHF/6-31+g\*\*, and MP2/6-31+g\*\* levels. The lowest energy structure found for neutral betaine is the same as that reported by Ratajczak.<sup>35</sup> Vibrational frequencies are obtained from force calculations at the RHF/6-31g\* level and are scaled by 0.91 prior to evaluation of zero-point energies and vibrational partition functions.<sup>36</sup>

The PA and GB of betaine were evaluated from these ab initio data using standard thermodynamic relationships.<sup>37</sup> For the protonation reaction



the PA is given by

$$PA = -\Delta H = -[E(MH^+) - E(M) - E(H^+) + \Delta PV] \quad (6)$$

$$= -[\Delta E_{\text{elec}} + \Delta E_{\text{zpe}} + \Delta(E_{298} - E_0) - E(H^+) + \Delta PV] \quad (7)$$

where  $E_{\text{elec}}$  is the self-consistent field electronic energy obtained from the Hartree-Fock model which also contains any energy correction due to electron correlations when the Möller-Plesset second-order perturbation (MP2) treatment is used.  $E_{\text{zpe}}$  is the vibrational zero-point energy,  $E_{298} - E_0$  is the energy contributions from translations, rotations, and vibrations at 298 K, and  $E(H^+)$  is the translational energy of a

(33) Griffin, L. L.; McAdoo, D. J. *J. Am. Soc. Mass Spectrom.* **1993**, *4*, 11–15.

(34) Gilbert, R. C.; Smith, S. C. *Theory of Unimolecular and Recombination Reactions*; Blackwell Scientific Publications: London, 1990.

(35) Latajka, Z.; Ratajczak, H. *Bull. Pol. Acad. Sci. Chem.* **1995**, *43*, 103–107.

(36) Hehre, W. J.; Radom, L.; Schleyer, P. R.; Pople, J. A. *Ab initio Molecular Orbital Theory*; Wiley: New York, 1986.

(37) McQuarrie, D. A. *Statistical Mechanics*; Harper Collins: New York, 1976.

**Table 1.** Measured Blackbody Infrared Radiative Dissociation Arrhenius Parameters and Product Ion Abundance for the Protonated Heterodimers of Betaine with Reference Bases

reference base <sup>a</sup>	structure	gas-phase basicity (kcal/mol) <sup>b</sup>	proton retention site <sup>c</sup>	measured log <i>A</i> <sup>d</sup>	measured <i>E</i> <sub>a</sub> (eV) <sup>d</sup>
DBU		242.6	DBU (100%)	9.8 ± 0.2	1.03 ± 0.02
DBN		240.3	DBN (78.6%)	10.6 ± 0.2	1.13 ± 0.02
betaine				10.6 ± 0.2	1.17 ± 0.02
TMG		238.4	betaine (81.7%)	8.5 ± 0.3	0.91 ± 0.03
TMDB		237.3	betaine (89.7%)	10.1 ± 0.3	0.95 ± 0.02
TMDP		235.7	betaine (100%)	9.5 ± 0.3	0.86 ± 0.02
DMPA		231.9	betaine (100%)	10.1 ± 0.3	0.97 ± 0.02
TBA		231.1	betaine (100%)	9.6 ± 0.3	0.90 ± 0.03

<sup>a</sup> Reference compounds *N,N*-dimethyl-4-pyridineamine (DMPA), tri-*n*-butylamine (TBA), *N,N,N',N'*-tetramethyl-1,4-diaminopropane (TMDP), *N,N,N',N'*-tetramethyl-1,4-diaminobutane (TMDB), 1,1,3,3-tetramethylguanidine (TMG), 1,5-diazobicyclo[4.3.0]non-5-ene (DBN), and 1,7-diazobicyclo[5.4.0]undec-7-ene (DBU). <sup>b</sup> Gas-phase basicity taken from the revised Lias scale.<sup>41</sup> <sup>c</sup> This is the product ion that predominantly retains the proton following dissociation; the value in parentheses is the percentage of total product represented by this ion. <sup>d</sup> Error is estimated from the standard deviation of a linear least-squares fit.

proton at 298 K. The GB is calculated from eq 8 using the calculated PA:

$$GB = -\Delta G = -[\Delta H - T\Delta S] = PA + T\Delta S \quad (8)$$

and

$$T\Delta S = T[S(\text{MH}^+) - S(\text{M}) - S(\text{H}^+)] \quad (9)$$

Translational, rotational, and vibrational entropy and energy values are calculated from the respective partition functions using standard methods of statistical mechanics after scaling harmonic vibrational frequencies evaluated at the RHF/6-31g\* level.

## Results

**Blackbody Dissociation Kinetics.** Rate constants for the dissociation of proton-bound dimers of betaine with itself and with a series of reference molecules were measured at cell temperatures between 93.7 and 219.7 °C. The dissociation kinetics of each dimer were measured over a 38–64 °C range between these temperatures. This range is ultimately limited by the kinetic window of the BIRD experiment using the current experimental apparatus.<sup>30</sup> The reference molecules with gas-phase basicities (GB) between 231.1 kcal/mol (TBA) and 242.6 kcal/mol (DBU) (Table 1) were selected to bracket the GB of betaine which has been previously measured by both Cooks<sup>19</sup> and Beauchamp.<sup>20</sup> The dissociation rate constants of the dimers were measured at cell pressures below  $2 \times 10^{-8}$  Torr. At this pressure, collisions do not influence the dissociation kinetics.<sup>15,26</sup> In this zero-pressure limit, ions are activated by absorption of blackbody photons generated by the vacuum chamber walls.

Dissociation of these proton-bound dimers results in the formation of protonated monomer ions exclusively over the temperature range investigated. No subsequent or competing dissociation processes were observed from either the dimer or monomer ion. Within the signal-to-noise ratio of these experiments (*S/N* > 100), the only observed protonated dissociation product of the heterodimers containing TMDP, DMPA, and TBA is betaine. For the proton-bound dimer of DBU and betaine (DBU·betaine), DBU retains the proton. For the other heterodimer ions, competition for retention of the proton between the dissociating molecules is observed. The relative abundance of these products averaged over all reaction delay times and temperatures is given in Table 1 for each base.

Unimolecular dissociation rate constants in the zero-pressure limit are obtained from the slope of a plot of  $\ln\{[D^+]/([D^+] + \sum[M^+])\}$  vs reaction time where  $[D^+]$  and  $[M^+]$  refer to dimer and monomer ion abundances, respectively. Kinetic plots for the unimolecular dissociation are shown in Figure 1 for three dimer ions which include the betaine homodimer (Figure 1b) and two bases that bracket the GB of betaine (Figure 1a,c). Excellent linear fits to the kinetics are obtained for all dimers. In addition, the y-intercepts for these data are zero. These results indicate that the internal energy distribution of the ion population has reached a steady state both prior to the reaction delay as well as over the entire reaction delay of these experiments.

**Zero-Pressure Limit Activation Parameters.** The Arrhenius activation energy (*E*<sub>a</sub>) and preexponential factor (*A*) for the dissociation of each dimer ion are obtained from the slope and y-intercept, respectively, of a plot of  $\ln(k)$  vs  $1/T$  plot (Figure 2). These values are given in Table 1. The error reported for

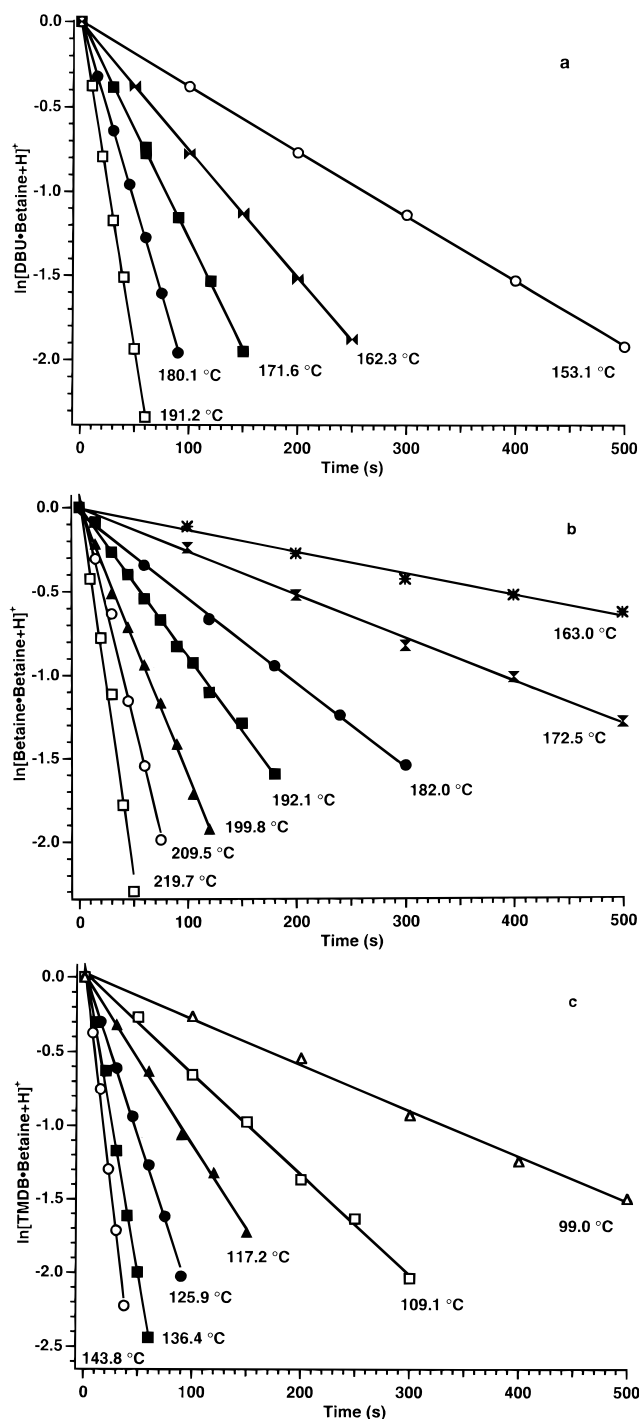


**Figure 1.** Blackbody infrared radiative dissociation data of the protonated dimers of (a) DBU·betaine, (b) betaine·betaine, and (c) TMDB·betaine fit to unimolecular kinetics at the temperatures indicated.

these parameters is calculated from the standard deviation of the slope and intercept of a linear least-squares fit to the data. This takes into account only random error. Potential sources of systematic error include a nonuniform chamber temperature and/or differences in detection efficiency for dimer and monomer ions. Although these errors may significantly change the measured dissociation rates, they only have a small effect on the temperature dependence of these rates; i.e., the experimental Arrhenius parameters are not strongly dependent on these values.<sup>9</sup>

With the exception of the TMG·betaine dimer, there is a strong correlation between the site of proton retention and the

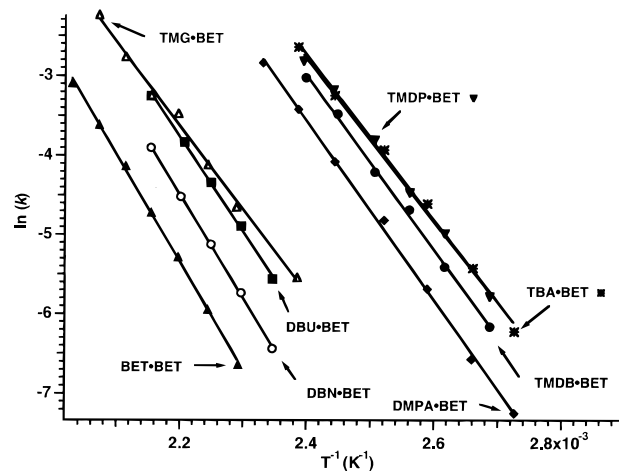


**Figure 2.** Zero-pressure limit Arrhenius plot for the dissociation of the protonated dimers of ( $\blacktriangle$ ) betaine, ( $\circ$ ) DBN·betaine, ( $\blacksquare$ ) DBU·betaine, ( $\triangle$ ) TMG·betaine, ( $\blacklozenge$ ) DMPA·betaine, ( $\bullet$ ) TMDB·betaine, ( $\blacktriangledown$ ) TMDP·betaine, and ( $\ast$ ) TBA·betaine.

temperature range required for the dissociation of these dimers. When betaine retains the proton, dissociation occurs at temperatures between 94 and 156 °C. When the reference base retains the proton, dissociation occurs at temperatures  $\sim 50$  °C higher for a similar  $k_{\text{uni}}$ . Both TMDP and TMDB can cyclize when protonated. TBA and DMPA, which have similar GB, cannot. The similar rates observed with these four bases indicate that the entropy of cyclization does not have a large effect on the absolute values of the dissociation rate constants under these conditions.

**Dimer Structures.** Minimized structures optimized at both the AM1 and PM3 levels for the ion–zwitterion and ion–molecule complexes of the TMG·betaine dimer are shown in Figure 3. Only one structure for the ion–zwitterion was found (**I**). However, several possible structures of comparable energy are possible for the ion–molecule complex (three structures, **II–IV**, shown). In **II**, the proton is shared between the basic sites of both molecules. This structure has the geometry most similar to that of the ion–zwitterion (**I**). However, this structure is the least stable of these ion–molecule complexes (**II–IV**). In **III** and **IV**, the base interacts with the quaternary ammonium end of the molecule which is charged. These structures are similar to the lowest energy ab initio structures modeled by Meot-Ner<sup>38</sup> for the clustering of quaternary ammonium ions with a range of solvent molecules. Structure **III** is the most stable of the ion–molecule complexes at both the AM1 and PM3 levels. However, **I** is 11.5 kcal/mol more stable by AM1 but is 2.2 kcal/mol less stable by PM3. For **I**, the binding energy is 1.55 eV at both AM1 and PM3. For **III**, this value is 1.05 and 1.66 eV at the AM1 and PM3 levels, respectively. Thus, the energies of the different structures calculated by AM1 and PM3 are inconsistent.

It should be noted that the semiempirical calculations are done in order to obtain vibrational frequencies and transition dipole moments used in the master equation modeling. In the modeling, these values are varied over a significantly wider range than the range of values obtained from the different structures. Thus, the value of  $E_0$  does not depend significantly on the choice of structure. The structures themselves obtained from the modeling do provide insight into the experimental results.

(38) Deakne, C. A.; Meot-Ner, M. *J. Am. Chem. Soc.* **1985**, *107*, 469–474.

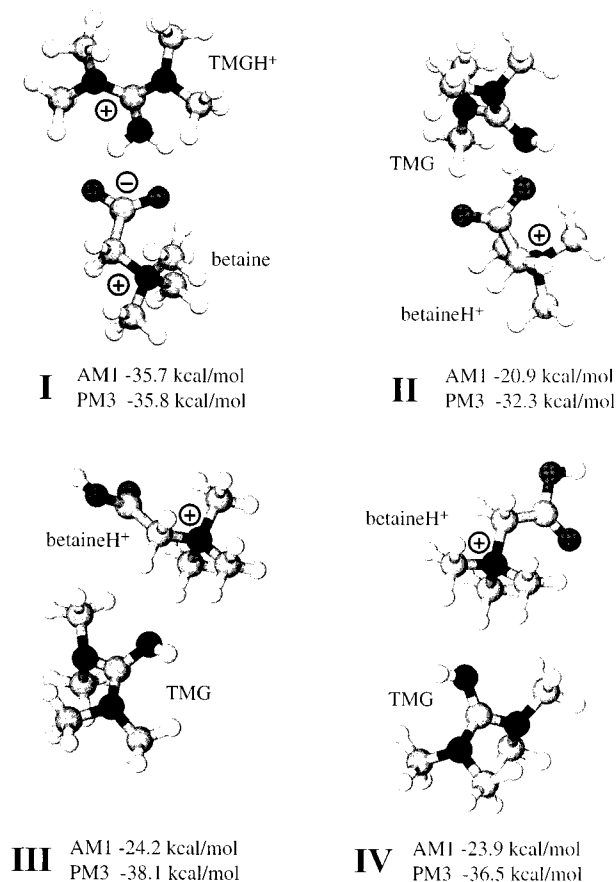
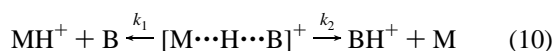


**Figure 3.** Minimized structures for TMG·betaine dimer and energies calculated at both the AM1 and PM3 semiempirical levels. Structure **I** is an ion-zwitterion complex; **II–IV** are ion-molecule complexes. All energies are referenced to the betaineH<sup>+</sup>·TMG exit channel.

## Discussion

**Measured GB of Betaine.** The kinetic method, first developed by Cooks and co-workers,<sup>39</sup> has been used to obtain gas-phase basicities of a variety of molecules.<sup>40</sup> This method is especially useful for compounds of low volatility which preclude the use of equilibrium measurements. In this method, the relative GB of a molecule is obtained from the product ion abundance ratios resulting from the dissociation of a proton-bound dimer of the molecule ([M]) with a series of reference bases ([B]):



The ratio of the product abundances is related to the difference in GB between the two compounds by eq 11:<sup>40</sup>

$$\ln([\text{MH}^+]/[\text{BH}^+]) \approx (\text{GB}_\text{B} - \text{GB}_\text{M})/RT_{\text{eff}} \quad (11)$$

A plot of the known GB of a series of reference bases vs the logarithm of the product abundance ratios gives a straight line with an *x*-intercept equal to the GB of [M] (assuming that there is no reverse activation barrier) and a slope that is proportional to the effective temperature (*T*<sub>eff</sub>).

The kinetic method plots for betaine dimers are shown in Figure 4. The abundance ratios are averaged over all temperatures and times for which BIRD kinetic data were obtained

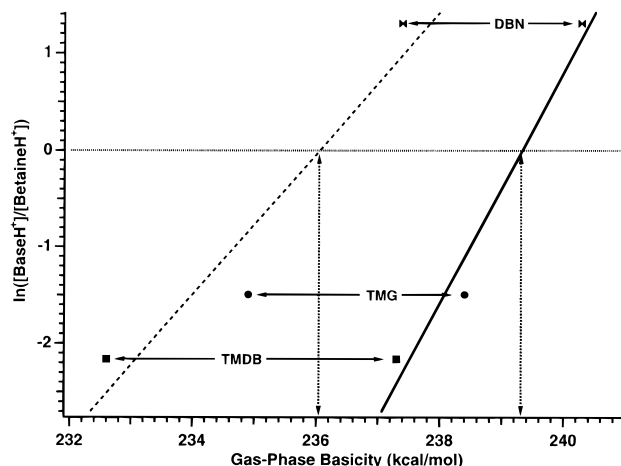


**Figure 4.** Kinetic method plots of the logarithm of the ratio of protonated monomers versus gas-phase basicity of reference compounds. Protonated betaine dimers were dissociated using blackbody infrared radiation in a Fourier transform mass spectrometer. Gas-phase basicity of betaine is determined using GB values for reference compounds from both the old (dotted line)<sup>21</sup> and the revised (solid line)<sup>41</sup> scales of Lias.

(~40–60 points acquired over several days). The experimental data are plotted with respect to the GB values of reference compounds using values from both the 1988 GB scale<sup>21</sup> (dashed line) and the revised 1997 scale<sup>41</sup> (solid line) of Lias. From the Figure 4 data, the GB of betaine anchored to the old and revised GB scale is  $236.0 \pm 1$  and  $239.3 \pm 1$  kcal/mol, respectively. This is the first demonstration of the kinetic method to obtain GB values using BIRD. Due both to the limited number of reference bases with similar GB to betaine and to the limited dynamic range of FTMS, competition for the proton between betaine and the base is observed only in the dissociation of betaine dimers with TMDB, TMG, and DBN. The product ratio of  $[\text{base}\cdot\text{H}^+]/[\text{betaine}\cdot\text{H}^+]$  changes from 0.23 to 3.68 when the reference base is TMG and DBN, respectively, an increase in GB of only 1.9 kcal/mol. These results clearly indicate that the GB of betaine is between that of those two bases.

Cooks and co-workers<sup>19</sup> previously reported a value for the GB of betaine as  $232.9 \pm 0.8$  kcal/mol (Lias, 1988 scale). This value is 3.1 kcal/mol lower than that reported here, and this difference is outside the combined error bars of these two experiments. Cooks' value was obtained by the kinetic method using the same reference bases used in this study. However, these experiments were done on a triple quadrupole mass spectrometer; dimer ions were dissociated using collisionally activated dissociation (CAD) with 6 eV collisions with argon. Two related factors account for the discrepancy in these two experiments; both the temperature of the ions as well as the kinetic window of these experiments differ significantly.

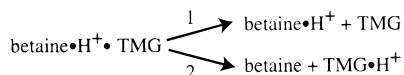
The time frame of kinetic measurements with BIRD in FTMS and CAD in a triple quadrupole instrument is 10–600 and 0.0001–0.001 s, respectively. For the TMG·betaine heterodimer, BIRD kinetics are measured at chamber temperatures between 419 and 483 K. This represents an upper limit to the effective ion temperature since the higher energy portion of the Boltzmann distribution is depleted under the conditions of this experiment. This is consistent with a *T*<sub>eff</sub> of 425 K obtained from the slope of the kinetic method plot (Figure 4). In contrast, the *T*<sub>eff</sub> in the CAD experiment was reported as 783 K.<sup>19</sup> The

(39) McLuckey, S. A.; Cameron, D.; Cooks, R. G. *J. Am. Chem. Soc.* **1981**, *103*, 1313–1317.

(40) Cooks, R. G.; Patrick, J. S.; Kotiaho, T.; McLuckey, S. A. *Mass Spectrom. Rev.* **1994**, *13*, 287–339.

(41) Hunter, E. P.; Lias, S. G. *NIST Standard Reference Database Number 69*; February 1997 Release, <http://webbook.nist.gov/chemistry/>.

## Scheme 1

**Table 2.** Product Ratio for the Dissociation of Protonated TMG·Betaine Dimer by Different Activation Methods<sup>a</sup>

activation method	maximum collision energy (eV)	ratio TMG:betaine
BIRD	NA	0.23
SORI-CAD	5.1	0.71
SORI-CAD	6.4	0.87
CAD	11.9	1.19

<sup>a</sup> Sustained off-resonance irradiation collisionally activated dissociation (SORI-CAD) applied for 2 s with 1.70 V peak-to-peak and for 1 s with 1.90 V p-p both at 771 Hz off-resonance. On-resonance collisionally activated dissociation applied for 10 ms at 107 mV p-p. Nitrogen collision gas at a pressure of  $2 \times 10^{-6}$  Torr was used in the CAD experiments.

discrepancy between Cooks' CAD and the BIRD experiments can be rationalized by a difference in transition state entropy between retention of the proton by betaine and the reference bases.

**Reaction Entropy.** To confirm that the reaction channels for formation of protonated base vs protonated betaine have different entropies, the energy dependence of the TMG·betaine dimer dissociation was investigated (Scheme 1). This dimer was dissociated with sustained off-resonance irradiation collisionally activated dissociation (SORI-CAD)<sup>42</sup> at two different peak-to-peak voltages and with on-resonance CAD. The ratios of  $[\text{TMG}\cdot\text{H}^+]/[\text{betaine}\cdot\text{H}^+]$  from these experiments are given in Table 2. This ratio increases from 0.23 for BIRD, the least energetic method, to 1.19 for on-resonance CAD, the most energetic method. In Cooks' experiment, this value is  $\sim 3.9$ . Despite the lower collision energy, the energy deposition in Cooks' experiment is higher than that in our on-resonance CAD experiment due to the higher collision rate in the quadrupole experiment which results in increased energy deposition into the ion prior to dissociation. These results show that the branching ratio for this dissociation process depends strongly on the internal energy of the ion. If the entropy of the two processes were the same, then the branching ratio would approach unity with increasing energy deposition. In the BIRD experiment ( $T_{\text{eff}} = 425$  K), the proton is retained primarily by betaine (82%). In the higher energy CAD experiments, the proton is retained primarily by TMG (80% in Cooks' CAD experiment). This indicates the retention of the proton by TMG is entropically favored. The GB values for betaine determined by the BIRD and quadrupole CAD methods are consistent. For dissociation of the TMG·betaine dimer, proton retention by TMG is entropically driven while retention of the proton by betaine is enthalpically favored. The origin of this relative entropy difference of the exit channels may be due to the properties of the base or may be due to the transition state of the ion-zwitterion channel occurring later along the reaction profile. A longer range electrostatic potential for the ion-zwitterion interaction may result in a looser transition state with relatively larger entropy than that of the ion-molecule interaction.

It is possible to obtain the magnitude of the relative entropy difference of the two reaction pathways using a modified version of Cooks' original kinetic method as demonstrated by Fenselau

(42) Gauthier, J. W.; Trautman, T. R.; Jacobson, D. B. *Anal. Chim. Acta* **1991**, *246*, 211–225.

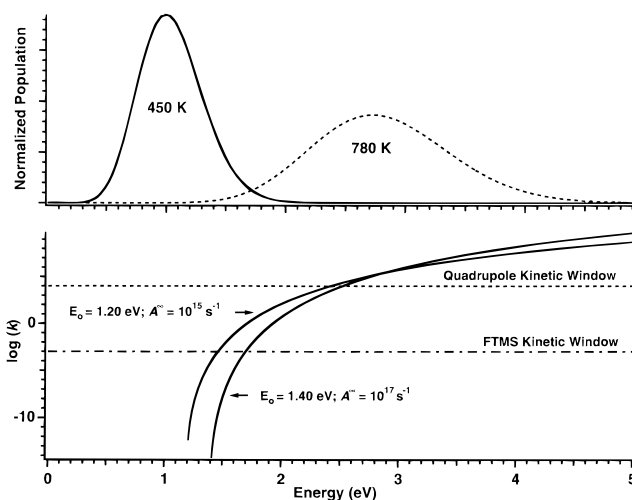


**Figure 5.** Calculated Boltzmann distributions for the TMG·betaine dimer at 450 K and 780 K (top) representing the average dissociation temperatures of blackbody infrared radiative dissociation in a Fourier transform mass spectrometer (FTMS) and collisionally activated dissociation in a quadrupole mass spectrometer, respectively. Wahrhaftig diagram (bottom) illustrating hypothetical dissociation processes, as indicated, for the protonated TMG·betaine dimer. Kinetic windows for FTMS (dotted-dashed line) and quadrupole mass spectrometer (dotted line) are displayed for reference.

and co-workers<sup>43</sup> and Cerda and Wesdemiotis.<sup>44</sup> In this method, branching ratios are measured at different effective temperatures using bases that are structurally similar. The reference bases used in this study are not structurally similar. However, it should be possible to obtain a rough estimate of the magnitude of the entropy difference by comparing the branching ratios in the BIRD experiment with those in Cooks' CAD experiment. A significant caution that needs to be emphasized is that, in order to obtain this value from the two different experiments, several assumptions must be made. These include the assumption that the product ion detection efficiencies in the two different instruments are the same, that the  $T_{\text{eff}}$  obtained from the kinetic method accurately reflects the internal energy of the ions, and that  $\Delta(\Delta H^\ddagger)$  has no temperature dependence. Within the limits of these approximations, the effective entropy difference between retention of the proton by TMG vs betaine is  $9 \text{ cal mol}^{-1} \text{ K}^{-1}$ .<sup>45</sup> This comparison is made using data at only two different effective temperatures. Clearly, using data at several different effective temperatures would provide a more accurate value.

A  $9 \text{ cal mol}^{-1} \text{ K}^{-1}$  difference in entropy between the transition states of these two channels corresponds to a 90-fold difference in REX limit Arrhenius preexponentials between the two dissociation channels. The effect of this entropy difference in conjunction with differences in  $T_{\text{eff}}$  and kinetic window on observed product branching ratios is illustrated in a Wahrhaftig plot<sup>46</sup> (Figure 5). The microcanonical dissociation constants are calculated using RRKM theory for two competing processes.

(43) Cheng, X.; Wu, Z.; Fenselau, C. *J. Am. Chem. Soc.* **1993**, *115*, 4844–4848.

(44) Cerda, B. A.; Wesdemiotis, C. *J. Am. Chem. Soc.* **1996**, *118*, 11884–11892.

(45) The effective entropy difference of the two competing reaction pathways for retention of the proton by TMG vs betaine is given by

$$\frac{RT_{\text{eff,CAD}} \ln([\text{MH}^+]/[\text{BH}^+]_{\text{CAD}}) - RT_{\text{eff,BIRD}} \ln([\text{MH}^+]/[\text{BH}^+]_{\text{BIRD}})}{T_{\text{eff,BIRD}} - T_{\text{eff,CAD}}}$$

(46) Futrell, J. H. *Gaseous Ion Chemistry and Mass Spectrometry*; John Wiley and Sons: New York, 1986.

**Table 3.** Calculated Gas-Phase Proton Affinity and Basicity of Betaine

basis set	proton affinity <sup>a</sup> (kcal/mol)	gas-phase basicity <sup>a</sup> (kcal/mol)
RHF/6-31g*	252.0	244.6
RHF/6-31+g**	256.2	248.8
MP2/6-31+g**	246.7	239.3
experiment		239.2

<sup>a</sup> Vibrational frequencies for the calculation of zero-point energies, enthalpy of heating to 298 K, and entropy contribution to gas-phase basicity evaluated at the RHF/6-31g\* level and scaled by 0.91.

One is enthalpically favored ( $E_o = 1.2$  eV,  $A^\infty = 10^{15}$  s<sup>-1</sup>) and is taken to represent the channel for retention of the proton by betaine. The other has a relatively larger entropic component ( $E_o = 1.4$  eV,  $A^\infty = 10^{17}$  s<sup>-1</sup>), i.e., a looser transition state, but a slightly higher dissociation energy and is taken to represent retention of the proton by TMG. The dissociation energies reflect those determined for the respective dissociation processes (vide infra), and the  $A^\infty$ -factors represent a range of loose transition states. Although not strictly accurate, Boltzmann distributions are calculated at 450 and 780 K to simulate the internal energy distribution of the BIRD and quadrupole CAD methods, respectively. The kinetic windows are determined by the slowest rate constants observable for these methods. For BIRD and quadrupole CAD, the slowest processes have dissociation constants of  $\sim 0.001$  and  $10\,000$  s<sup>-1</sup>, respectively. At higher ion temperatures, the process with the larger  $A^\infty$  has a larger rate constant, so this process is favored at the higher temperatures of the CAD process. At the lower temperatures of the BIRD method, the process with the lower dissociation energy ( $E_o$ ) is favored. Both activation methods yield an accurate GB for betaine at the temperature of the experiment.

In principle, the BIRD technique can be used to determine the entropy difference in reaction pathways from the temperature dependent change in the product branching ratio. However, no temperature dependence outside experimental error was observed for the product ion ratios for these dimers. This is most likely due to the limited temperature range (64 °C for TMG). The difference in  $T_{\text{eff}}$  between Cooks' CAD experiment and the BIRD experiment is 6 times larger than the temperature range of the BIRD experiment alone. Thus, it should be possible to obtain a more accurate value of the entropy difference by comparing the BIRD and CAD data within the limits of the assumptions stated previously.

**Calculated GB of Betaine.** The values of PA and GB calculated at increasing levels of theory are shown in Table 3. Polarization functions on both heavy atoms and hydrogens are required to accurately model thermodynamic functions for small molecules, and diffuse functions generally reproduce experimental values more accurately for negative ions.<sup>36</sup> Since neutral betaine is a zwitterion, the addition of these functions should provide more accurate values for GB. The effects of electron correlation can be considerable for protonation reactions. Thus, it is expected that the PA and GB values calculated at the MP2/6-31+g\*\* level are the most reliable. At this level, the GB is calculated to be 239.3 kcal/mol at 298 K. Changing the scaling factor for the frequencies (RHF/6-31g\*) from the established value of 0.91<sup>36</sup> to either 0.90 or 0.92 results in a  $\leq 0.1$  kcal/mol change in the calculated GB. Even a scaling factor of 1.0 results in a  $< 1$  kcal/mol change in GB. Thus, errors in the frequencies are unlikely to be a significant source of error in these calculations. However, higher level calculations are necessary to show whether the GB has converged to the true value. Nevertheless, the excellent agreement with our experimental

value (239.2 kcal/mol) using the revised GB scale is gratifying. All subsequent GB values are referenced to this revised scale.

**Master Equation Modeling of the Experiment.** The threshold dissociation energies ( $E_o$ ) for these dimers can be obtained from the measured zero-pressure limit Arrhenius parameters using master equation modeling. Included in this model are calculated rate constants for radiative absorption, radiative emission, and dissociation. Three parameters ( $\mu$ ,  $A^\infty$ , and  $E_o$ ) are adjusted in the master equation model. The first two parameters are varied over a reasonable range to estimate the uncertainty in the absolute radiative rates and the transition state entropy, respectively.  $E_o$  is the value of interest and is adjusted within the range of the first two parameters to fit the experimental data. These three parameters are coupled. For example, a decrease of  $E_o$  results in an increase in the modeled  $k_{\text{uni}}$ , but a simultaneous decrease in either  $A^\infty$  or the transition dipole scaling factor can offset this change. However, the relative temperature dependence of these parameters may not be the same, and different modeled  $E_a$  and  $A$  values may result. Thus, reasonable fits can only be obtained over a relatively narrow range of  $E_o$  values.

Two criteria are used to determine if a fit is within the limits of our model. First, the modeled  $E_a$  and  $A$  must both fall within the error bars of the measured values. Second, the calculated  $k_{\text{uni}}$  must be within a factor of 2 of the experimental values. Reproducibility of absolute rate constants is significantly better than a factor of 2, but this range should account for systematic error that may be present in either the temperature calibration or the relative detection efficiency of the ions. The error reported for  $E_o$  is determined from the highest and lowest calculated values that will fit the experimental data, within these criteria.

The effects of varying each of the adjustable fitting parameters in the master equation model on  $k_{\text{uni}}$ ,  $E_a$ , and  $A$  for the proton-bound dimers of *N,N*-dimethylacetamide (*N,N*-DMA) and amino acids have been described previously.<sup>25</sup> The value of  $E_o$  is the most critical factor for obtaining accurate fits to the experimental  $E_a$ . The exquisite sensitivity of the kinetics to the value of  $E_o$  makes possible extraction of this value from the zero-pressure data with high precision. For these calculations,  $E_o$  was initially changed in 0.05 eV increments from 1.00 to 1.60 eV to bracket the range of  $E_o$  that fit the data. A finer grain step size (0.01 eV) was then used to pinpoint the limits more precisely. A detailed description of the range of values of  $\mu$  and  $A^\infty$  that were used follows.

Dissociation of proton-bound dimers is entropically favored and characterized by a "loose" transition state ( $A^\infty \geq 10^{14}$  s<sup>-1</sup>). There is clear evidence that the entropy of the transition for dissociation depends on which species retains the proton (vide supra). In addition, the reference bases used to form proton-bound dimers with betaine in this study are structurally dissimilar and are likely to have different transition state entropies for dissociation. For example, TMDP and TMDB have two polar groups that can interact with the charge in the complex. Dissociation of the complex can open up internal rotations if these molecules do not retain the charge. This would result in a large activation entropy. In contrast, DBN and DBU are bicyclic compounds that have no active internal rotors in either the reactant or transition state. To take into account the different transition state entropies possible for these complexes, four transition state frequency sets were constructed for each dimer spanning the loose range of rapid energy exchange limit Arrhenius preexponential factors ( $10^{14.0}$ ,  $10^{15.0}$ ,  $10^{16.2}$ , and  $10^{17.4}$  s<sup>-1</sup>). The latter value is comparable to the largest  $A$  factor



reliably measured for neutral molecule dissociations and should be a reasonable upper limit for dissociation of these ionic complexes as well.<sup>34,47</sup>

Accurate transition dipole moments are critical for modeling the experimental  $k_{\text{uni}}$  but have only a minor effect on the Arrhenius parameters. Experimental values for the systems investigated here are not available. Values of  $\mu$  calculated at the ab initio level are typically 1.4 times larger than experimental values for small neutral molecules, but compare more favorably for small ions.<sup>25,29,48</sup> A direct comparison of absolute transition dipole moments calculated at the AM1 semiempirical level with experimental integrated line intensities is not available, but AM1 calculations are fast and efficient at reproducing the expected relative transition intensities to a fairly high level of accuracy. For proton-bound dimers of amino acids and analogues, both experimental results and ab initio calculations indicate that the semiempirically derived values are approximately a factor of 3 too small.<sup>25,49</sup> For protonated betaine dimer, the integrated absorption rates calculated at the ab initio RHF/6-31g\* level are  $\sim 3.3$  times larger ( $\mu \sim 1.8$  times larger) than those calculated with AM1 values. However, due to the structural differences in the reference bases used, a single scaling factor is not expected. A scaling factor between 1 and 3 was used in these calculations and should account for the uncertainty in the absolute radiative rate constants for these dimers.

The effects of these parameters on the modeling are illustrated for the protonated betaine-TMG dimer which has measured zero-pressure limit Arrhenius parameters of  $0.91 \pm 0.03$  eV and  $10^{8.5 \pm 0.3} \text{ s}^{-1}$ . Figure 6 shows the experimental data and the results of these calculations. For clarity, only those fits that are at the limits of acceptability are included (best fits are not on the graph). The experimental data can be fit using a  $\mu$  scaling factor of 1 if the proton is on TMG (Figure 6a) and 2 if the proton is on betaine (Figure 6b), independent of  $A^\infty$ . No fits could be obtained for the other values. For  $A^\infty$  between  $10^{15}$  (dashed lines) and  $10^{17.4} \text{ s}^{-1}$  (dotted lines),  $E_0$  must be between 1.25 and 1.35 and 1.28 and 1.38 eV for a  $\mu$  scaling factor of 2 and 1, respectively, to fit the measured Arrhenius data to within the precision of the experiment. The value of  $E_0$  we report for this dimer is  $1.32 \pm 0.07$  eV. The error bars include uncertainty in both the experiment as well as the modeling. It is emphasized that the latter includes uncertainties in both the transition state entropy and the radiative rate constants. Even with these large uncertainties, values of  $E_0$  can still be obtained for a variety of proton-bound dimers with high accuracy.<sup>25,49</sup> For example, the binding energy of the proton-bound dimer of *N,N*-dimethylacetamide obtained by this method is nearly identical to that obtained by high-pressure mass spectrometry.<sup>25</sup> The values of  $E_0$  obtained by this modeling and the range of the fitting parameters ( $A^\infty$  and  $\mu$  scaling factor) are reported in Table 4 for each of the protonated betaine-base dimers investigated.

**Binding Energies.** To the extent that the reverse activation barriers for these reactions are negligible, the values of  $E_0$  we obtain from the master equation analysis should be equal to the binding energies. With the exception of the TMG-betaine dimer, a strong correlation is observed between the binding energy and the site of proton retention. The binding energy is  $\sim 1.4$  and  $\sim 1.2$  eV when the proton remains on the reference

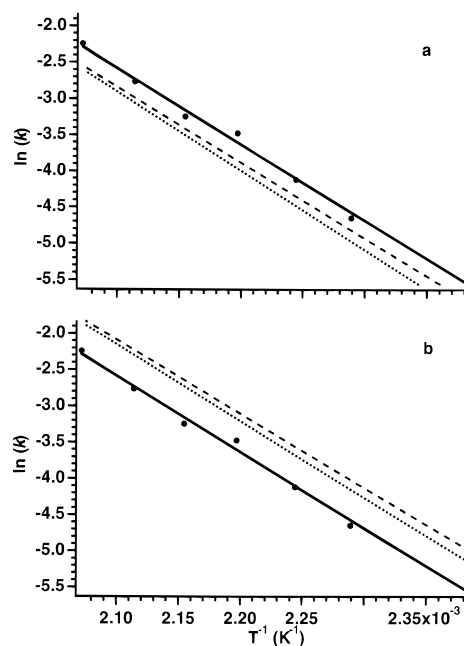


**Figure 6.** Zero-pressure limit Arrhenius plots of the experimental data (●) and limiting case master equation modeled fits for the dissociation of protonated TMG-betaine dimer with (a) transition dipole moments calculated at the AM1 level with  $A^\infty = 10^{15.0} \text{ s}^{-1}$  and  $E_0 = 1.28$  eV (dashed line) and  $A^\infty = 10^{17.4} \text{ s}^{-1}$  and  $E_0 = 1.38$  eV (dotted line) and (b) transition dipole moments 2 times larger than AM1 values with  $A^\infty = 10^{15.0} \text{ s}^{-1}$  and  $E_0 = 1.25$  eV (dashed line) and  $A^\infty = 10^{17.4} \text{ s}^{-1}$  and  $E_0 = 1.35$  eV (dotted line). These master equation fits represent the maximum acceptable limit within the error of the experiment.

base and on betaine, respectively. Betaine has a large permanent dipole ( $\mu = \sim 12$  D). The dipole moments for the reference bases are significantly smaller ( $\mu < 3.5$  D).<sup>50</sup> The  $\sim 0.2$  eV higher binding energy when the base retains the charge is due to a stronger ion-dipole interaction when betaine remains electrically neutral, i.e., a zwitterion, throughout the reaction profile.

Figure 7 illustrates the effects of the basicity of the reference bases on the reaction potential. For the DBU-betaine dimer (Figure 7a), the more stable ion-zwitterion complex is favored and the dissociation occurs via the more enthalpically favorable dissociation pathway ( $1.35 \pm 0.08$  eV), reflecting the 3.4 kcal/mol difference in GB between betaine and DBU. For the DBN-betaine dimer (Figure 7b), the difference in energy of the competing exit channels is only  $\sim 1.1$  kcal/mol.<sup>51</sup> The ion-zwitterion complex is still the most favored structure, but both products are observed due to their similar energies. Both channels will contribute to the measured binding energy, but the 1.1 kcal/mol difference in product ion energy cannot be distinguished within the error of the measured  $E_0$  of  $1.40 \pm 0.08$  eV.

For the TMG-betaine dimer (Figure 7c), the relative energies of the exit channels are the reverse of the previous example. Dissociation to form protonated betaine is  $\sim 0.8$  kcal/mol lower in energy than the protonated base. On the basis of the higher binding energy, the dissociating population is still primarily the ion-zwitterion structure at the temperatures used in the BIRD experiment, even though the ion-zwitterion dissociation channel is not the favored pathway for dissociation. The binding energy of  $1.32 \pm 0.07$  eV measured for this complex is lower than

(47) Benson, S. W. *Thermochemical Kinetics. Methods for the Estimation of Thermochemical Data and Rate Parameters*; John Wiley & Sons: New York, 1968.

(48) Keim, E. R.; Polak, M. L.; Owrutsky, J. C.; Coe, J. V.; Saykally, R. J. *J. Chem. Phys.* **1990**, *93*, 3111–3119.

(49) Jockusch, R. A.; Williams, E. R. *J. Phys. Chem. A*, submitted for publication.

(50) Dipole moments are calculated at the AM1 semiempirical level.

(51) For betaine and all the bases, except TMDP and TMDB, the relative entropy factors are all within 2 kcal/mol.

**Table 4.** Master Equation Model Fitting Parameters for Extracting Threshold Dissociation Energy from Measured Arrhenius Values

reference base	modeled proton site	modeled photon absorption rate (s <sup>-1</sup> ) <sup>a</sup>	modeled E <sub>0</sub> range (eV)	modeled log A range	E <sub>0</sub> (eV)
betaine	betaine	3.8	<i>b</i>	<i>b</i>	1.45 ± 0.05
		15.2	1.40–1.50	14.0–17.4	
		34.2	<i>b</i>	<i>b</i>	
DBU	DBU	3.8	1.33–1.43	14.0–17.4	1.35 ± 0.08
		15.1	1.27–1.30	14.0–15.0	
		34.0	<i>b</i>	<i>b</i>	
DBN	DBN	3.8	1.43–1.48	16.2–17.4	1.40 ± 0.08
		15.0	1.33–1.42	14.0–16.2	
		33.9	<i>b</i>	<i>b</i>	
TMG	betaine	2.3	<i>b</i>	<i>b</i>	1.32 ± 0.07
		9.0	1.25–1.35	15.0–17.4	
		20.3	<i>b</i>	<i>b</i>	
TMG	TMG	3.9	1.28–1.38	15.0–17.4	
		15.8	<i>b</i>	<i>b</i>	
		35.5	<i>b</i>	<i>b</i>	
TMDB	betaine	1.1	<i>b</i>	<i>b</i>	1.22 ± 0.04
		4.4	1.18–1.25	15.0–17.4	
		10.0	1.20–1.23	15.0–16.2	
TMDP	betaine	1.2	<i>b</i>	<i>b</i>	1.17 ± 0.03
		4.9	1.16–1.18	15.0	
		10.9	1.14–1.20	15.0–17.4	
DMPA	betaine	1.8	<i>b</i>	<i>b</i>	1.21 ± 0.05
		7.3	<i>b</i>	<i>b</i>	
		16.4	1.16–1.25	15.0–17.4	
TBA	betaine	0.8	<i>b</i>	<i>b</i>	1.20 ± 0.06
		3.5	1.15–1.25	15.0–17.4	
		7.8	1.14–1.18	15.0–16.2	

<sup>a</sup> Photon absorption rate calculated at the central experimental temperature assuming only the  $\nu = 0$  vibrational state is occupied. Average energy of the absorbed photon is between 1000 and 1500 cm<sup>-1</sup> depending on both the temperature and the oscillator strength of the transitions. <sup>b</sup> A fit was not possible with these parameters.

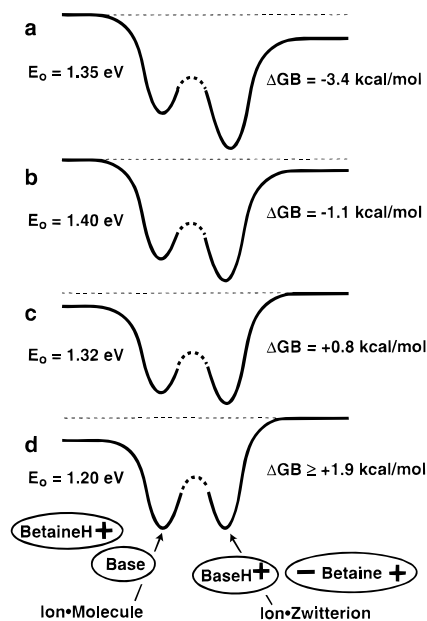


**Figure 7.** Energy diagrams for the dissociation of proton-bound dimers of betaine and reference bases of decreasing gas-phase basicity: (a) DBU, (b) DBN, (c) TMG, (d) TMDB, TMDP, DMPA, and TBA. The  $\Delta$ GB values reported correspond to the differences in gas-phase basicity between betaine and the reference bases. The measured value of  $E_0$  for betaine with each base is also indicated on the diagram.

that for DBN and DBU and, in part, may reflect the lower exit barrier height of the ion–molecule product pathway. However, within the error bars, these values are indistinguishable.

When betaine is more basic than the reference base by  $\sim 2$  kcal/mol or more (Figure 7d), the binding energy is  $\sim 1.20 \pm$

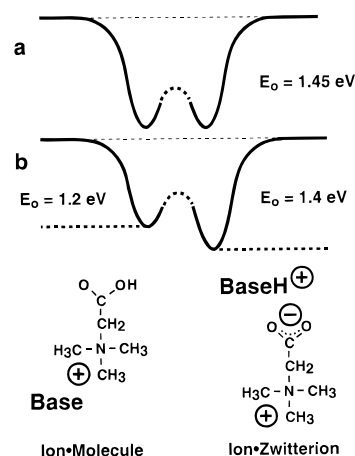


**Figure 8.** Energy diagrams for the dissociation of proton-bound dimers of betaine with a base of identical gas-phase basicity: (a) homodimer of betaine and (b) a heterodimer of betaine with an equally basic nonzwitterionic compound.

0.05 eV (average value for TMDB, TMDP, DMPA, and TBA). This indicates that the ion–molecule conformation of the dimer is more favored. There are significantly more similar energy structures for the ion–molecule conformation than for the ion–zwitterion structure. Thus, this ion–molecule conformation is somewhat entropically favored.

The energy diagrams for dimers with constituents of equal GB are shown in Figure 8. The simplest case is illustrated for the betaine homodimers (Figure 8a). The reaction profile is symmetrical and has a measured  $E_0$  of  $1.45 \pm 0.05$  eV. Heterodimers with constituents of equal GB have an asymmetric potential. A hypothetical example is shown in Figure 8b. To the extent that  $E_0$  values measured for the betaine heterodimers accurately reflect the true binding energies of these complexes, the exit channel leading to a protonated reference base has a binding energy of  $\sim 1.4$  eV whereas the dissociation channel from the ion–molecule complex to protonated betaine as the product has an  $E_0$  of  $\sim 1.2$  eV. The difference in these values should be approximately equal to the difference in energy of an ion–zwitterion vs ion–neutral complex. Thus, the ion–zwitterion complex should be the dominant structure in the gas phase.

As discussed earlier, the energies of the ion–zwitterion and ion–neutral complexes calculated at the AM1 and PM3 semiempirical levels are inconsistent. In addition, both methods provide energies that are inconsistent with the experimental values. Interestingly, the AM1 derived binding energies are closer to these experimental values than those from PM3. AM1 values appear to overestimate the relative stability of the ion–zwitterion vs ion–molecule complex, whereas this difference is significantly underestimated by PM3. The experimental results also suggest that the most stable structure of an ammonia–betaine dimer should be an ion–molecule complex, not an ion–zwitterion as predicted by PM3,<sup>3</sup> due to the significantly lower GB of ammonia.

## Conclusions

Dissociation energies of proton-bound dimers of betaine with neutral molecules of similar gas-phase basicity were obtained from master equation modeling of measured BIRD kinetics. For bases of higher or comparable gas-phase basicity, the binding energies are  $\sim 1.4$  eV. For bases that are  $\sim 2$  kcal/mol or more less basic than betaine, betaine retains the charge and the binding energy is  $\sim 1.2$  eV. For these bases, the most stable structures

are ones in which the base interacts with the quaternary nitrogen end of betaine which retains the charge. In contrast, for bases of comparable or higher gas-phase basicity, the zwitterionic structure is more stable. The higher binding energy of these ion-zwitterion complexes is consistent with a significantly stronger ion-dipole interaction due to the large dipole moment of neutral (zwitterionic) betaine. For a base with a gas-phase basicity that is lower by  $\sim 1$  kcal/mol, the measured binding energies indicate that the ion-zwitterion complex in which the base is protonated is more stable, even though the ion-molecule dissociation pathway in which betaine retains the proton is favored.

In addition to binding energies, the gas-phase basicity of betaine was obtained from the BIRD data using the kinetic method and was found to be  $239.2 \pm 1.0$  kcal/mol. This value is in excellent agreement with the value of 239.3 kcal/mol at 298 K obtained from ab initio calculations at the MP2/6-31+g\*\* level. The gas-phase basicity reported here is  $\sim 3$  kcal/mol

higher than that reported previously.<sup>19</sup> This difference is attributed to a difference in entropy for dissociation via an ion-molecule vs ion-zwitterion channel. Due to the lower ion internal energy and longer time frame of the BIRD experiment, gas-phase basicities obtained by BIRD should be closer to those at standard temperature.

Increasing evidence indicates that zwitterions and salt bridges play an important role in the gas-phase structure and reactivity of larger biomolecules. The results with betaine presented here indicate that the measurement of binding energies of bioion-neutral complexes could be a useful probe for the presence of zwitterions in the gas phase.

**Acknowledgment.** We are grateful for generous financial support provided by the National Science Foundation (Grant CHE-9258178) and the National Institutes of Health (Grant 1R29GM50336-01A2).

JA972527Q